ISSN (Online) 2456 -1304

International Journal of Science, Engineering and Management (IJSEM)
Vol 5, Issue 2, February 2020

Mathematical Modeling of a Rope Vortex in Swirling Flows

[1] Elena Corina Cipu
[1] Department of Applied Mathematics, Faculty of Applied Sciences, University POLITEHNICA of Bucharest, Romania

Abstract: **- Appearance of a rope vortex in swirling flows under the runner of Kaplan and Francis hydraulic turbine are studied. The ratio between the two lengths, that is the length of the rope vortex type and the height of the column water in which it appears, H , is specified. The calculus is made for the case of a curve on a surface described by a half spindle surface and frustum of a cone. We have compute the ratio between the length of the rope vortex and the characteristic length H .**

Keywords: vortex rope, swirling flows, frustum of a cone, spindle surface

1. INTRODUCTION

The swirling flow developing in the Francis turbine draft tube under the part load operation leads to pressure fluctuations usually in the range of 0.2 to 0.4 times the runner rotational frequency resulting from the so-called vortex breakdown (Kuibin et al, 2011, [7]; Susan-Resiga et al, 2009, [11]; Ciocan et al, 2007, [5]). For the low cavity number, the flow features a cavity vortex rope animated with precession motion.

Pressure fluctuations may appear in a higher frequency range of 2 to 4 times the runner rotational speed and feature modulations with vortex rope precession.

The vortex rope is located on the border between the mainstream swirl and the stagnant central region (see Susan-Resiga et al, 2009, [11]). The destructive effects of the cavitation phenomenon which appears under the rotors of the hydraulic turbines are well known (Baran et al, 2005, [4]; Bosioc et al., [3]).

Until now different researchers tried to analyse the problem using numerical methods (Baoshan Zhu et al, 2014, [2]; Kurosava et al, 2006, [8]; Susan-Resiga et al, 2006, [10]; Zhow et al, 2006, [12]). The application of numerical methods requires extensive work and much time to characterize the depression zone in swirling flows. There appear as a necessity the elaboration of an analytical approach to estimate more generally, faster and less costly the main characteristics of the depression zone. This is necessary to avoid the excess of the air, eventually outside of the depression zone.

The effect could be dangerous by the introduction of undesired perturbations. In this work we try to predict this phenomenon and, for consequence, to give more information concerning the design (including the volumes dimension and the geometrical characteristics) of the air device.

The vortex rope features elliptical cross section and is animated by self-rotation. We shall suppose that the section is so small that it might be approximate with a point, searching for realistic approximations of the curves that describe its motion. The ratio between the two lengths, that is the length of the rope vortex type and the height of the column water in which it appears , H , will be determined.

2. PARAMETRIZATION OF THE CURVE DETERMINED BY THE ROPE VORTEX

We shall consider two cases for the calculus of the length of the rope vortex, named L . In first case we suppose that the curve is on a surface cone, as is one obtained by experimental study (see [6], [9], Fig 1) and in second case that the curve is on a spindle surface (suggested also by simulations, as it is shown in Fig. 3 and Fig. 4). We shall compute the ratio $\mathrm{r} = L/H$ with L as the length of the rope vortex.

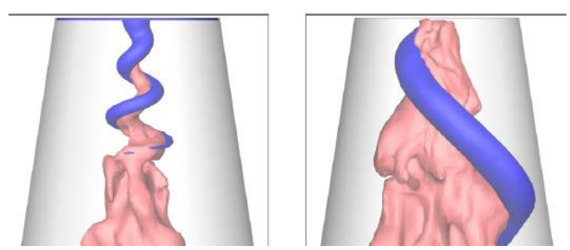

See [6] , pag 7

ISSN (Online) 2456 -1304

International Journal of Science, Engineering and Management (IJSEM)
Vol 5, Issue 2, February 2020

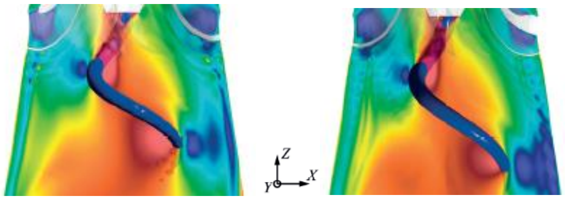

See [9], pag 90

Fig. 1 Isopresure surface representing vortex rope and isovelocity surface

(a)We suppose that the rope vortex is lying on a frustum of a cone, determined by radius r_1, r_2 and high $\mathrm{H} = \boldsymbol{H}\,\mathrm{p}$,where for p=1 one obtains the entire cone. The parametric equations are:

$$\begin{cases} x = \rho\cos\theta, y = \rho\sin\theta, \quad \rho = r_1 + (r_2 - r_1)\left(1 - \dfrac{z}{\boldsymbol{H}}\right) \\ z = \dfrac{\boldsymbol{H}\ p}{2\pi m}\theta, \quad \theta \in [0, 2\pi m], m \in \mathbf{N} \end{cases}$$

(1)

precise the number of rotations of the rope, as is shown in Fig.2.

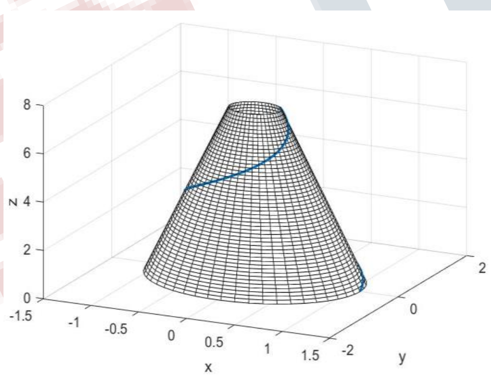

(a)

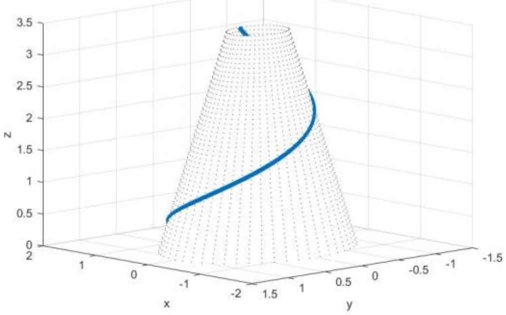

(b)

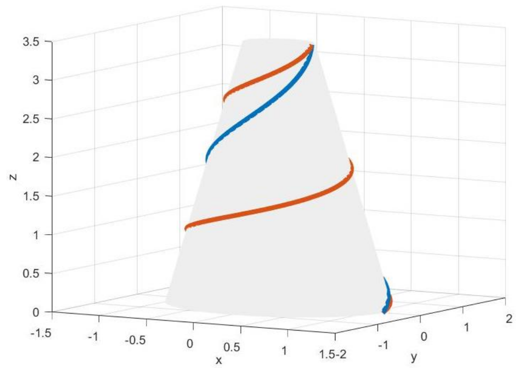

(c)

Fig. 2. Frustum of a cone (a) $r_2 = 1.2$, $r_1 = 0.2$, $\boldsymbol{H} = 2.1$;

(b) $r_2 = 1.1$, $r_1 = 0.35$, $\boldsymbol{H} = 3.4$; (c) same as (b) m=1,m=2, respectively

(b)We suppose that the rope vortex is lying on a spindle surface obtained by a rotation of a parabola $\mathrm{z}_0\mathrm{z}(\boldsymbol{H}\text{-}\mathrm{z})$, with $\mathrm{R} = \boldsymbol{H}\,\mathrm{k}$, $\mathrm{k} \in (0, \mathrm{p})$. The maximum value in $\mathrm{z} = \dfrac{\boldsymbol{H}}{2}$ corresponding to the notation $\mathrm{z}_0 = \dfrac{4\mathrm{R}}{\boldsymbol{H}^2}$. The high of the rope vortex is $\mathrm{H} = \boldsymbol{H}\,\mathrm{p}$, for p=1 one obtains the entire spindle surface. In Fig.3 is represented the rope vortex for p=0.5; p=2/3 and p=0.75 respectively.

The parametric equations of the rope vortex are :

$$\begin{cases} x = z_0 z(\boldsymbol{H}\text{-}z)\cos\theta \\ y = z_0 z(\boldsymbol{H}\text{-}z)\sin\theta, \quad \theta \in [0, 2\pi m], m \in \mathbf{N} \\ z = \dfrac{\boldsymbol{H}\ p}{2\pi m}\theta \end{cases} \qquad (2)$$

where for $\theta \in [0, 2\pi]$, (2) expresses a complete rotation of a point moving on the curve.

International Journal of Science, Engineering and Management (IJSEM)
Vol 5, Issue 2, February 2020

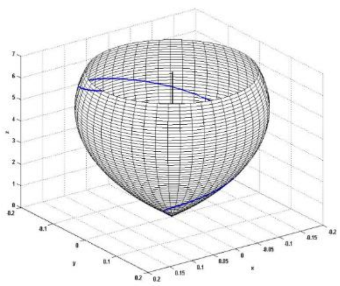

(a)

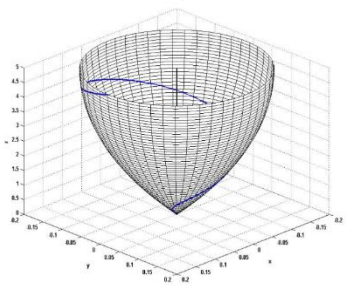

(b)

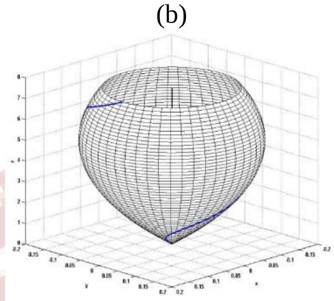

(c)

Fig. 3. Spindle surface (a) p=0.5; (b) p=2/3; (c) p=0.75 respectively

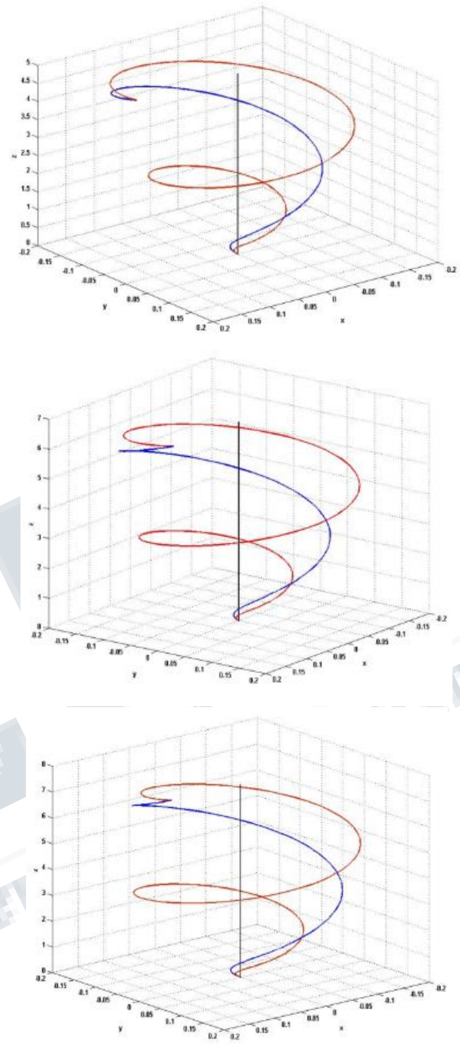

Fig. 4 m=1 and m=2 for (a) p=0.5,(b) p=2/3 and (c) p=0.75 respectively.

3. LENGTH CALCULUS FOR CURVE DETERMINED BY THE ROPE VORTEX

We use for the length of the curve classical formulas

$$\boldsymbol{L}=\int_C ds\,,\; ds=\sqrt{x'(\theta)^2+y'(\theta)^2+z'(\theta)^2}\,d\theta. \quad (3)$$

(a) In case of a frustum of a cone one obtains making the calculus for the length as in (3) for m=1, one obtains

$$\boldsymbol{L}=\boldsymbol{H}\,l_{1,k}(p)=\int_0^{2\pi}\sqrt{A_k^2+p_{1,k}(t,p)^2}\,dt$$

with $$p_1(t,p)=\frac{r_1}{\boldsymbol{H}}+k\left(1-\frac{p}{2\pi}t\right),\; A_k=\frac{p}{2\pi}\sqrt{k^2+1}\,,\; k=(r_2-r_1)/\boldsymbol{H} \qquad (4)$$

and

International Journal of Science, Engineering and Management (IJSEM)
Vol 5, Issue 2, February 2020

$$\boldsymbol{L} = \boldsymbol{H}\, l_{m,k}(p) = \int_0^{2\pi m} \sqrt{A_{m,k}^2 + p_{m,k}(t,p)^2}\, dt$$

with

$$p_{m,k}(t,p) = \frac{r_1}{\boldsymbol{H}} + k\left(1 - \frac{p}{2\pi m} t\right). \quad A_{m,k} = \frac{p}{2\pi m}\sqrt{k^2+1} \qquad (5)$$

The explicit calculus could be made in this case,

$$l_{m,k}(p) = \frac{2\pi m}{p}\left(\ln\left(\frac{u_2 + \sqrt{u_2^{\,2} + A_{m,k}^2}}{u_1 + \sqrt{u_1^{\,2} + A_{m,k}^2}}\right) + \frac{u_2\sqrt{u_2^{\,2} + A_{m,k}^2} - u_1\sqrt{u_1^{\,2} + A_{m,k}^2}}{2}\right) u_1 = \frac{r_1}{\boldsymbol{H}} + k(1-p),\ u_2 = \frac{r_2}{\boldsymbol{H}} \quad (6)$$

(a) In case of a spindle surface one obtains making the calculus for the length as in (3) for m=1, one obtains

$$r_{1,k}(p) = \int_0^1 \sqrt{1 + 16k^2 p_1(t,p)}\, dt$$

and

$$p_1(t,p) = 1 - 4pt + 4(p^2 + \pi^2)t^2 - 8\pi^2 p t^3 + 4\pi^2 p^2 t^4. \qquad (7)$$

Generalized relations for any m are:

$$r_{m,k}(p) = \int_0^1 \sqrt{1 + 16k^2 p_m(t,p)}\, dt \qquad (8)$$

$$p_m(t,p) = 1 - 4pt + 4(p^2 + \pi^2 m^2)t^2 - 8\pi^2 m^2 p t^3 + 4\pi^2 m^2 p^2 t^4.$$

To obtain numerical values for the correlation $\mathrm{r}_{m,k}(\mathrm{p})$ we consider the variable p in the range of 0.60 and 1 with a step of 0.05 and integrate (7) – (8) for $\mathrm{k} = \frac{\mathrm{R}}{\boldsymbol{H}} = \frac{0.18}{10}$ and m=1, m=2 using a Taylor expansion for $\mathrm{p}_m(\mathrm{t},\mathrm{p})$ in the vicinity of point t_0. Were used at least 200 terms in the expansion and the computing error is less than $O(\mathrm{t}^{-50})$. The results shown in Fig.5.

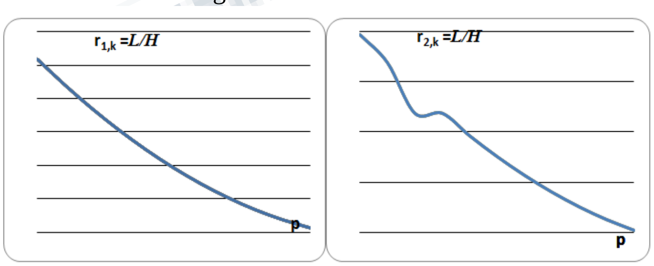

Fig.5 The ratio of the lengths of the rope vortex versus the ratio of the two heights $p = \frac{\boldsymbol{H}}{\mathrm{H}}$, $p \in [0.6, 1]$**, step=0.05**

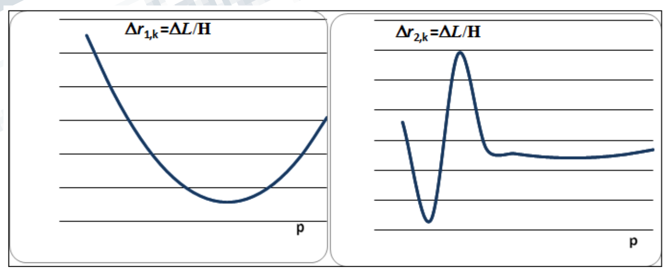

Fig.6 The ratio variation of the lengths of the rope vortex versus the rapport of the two heights

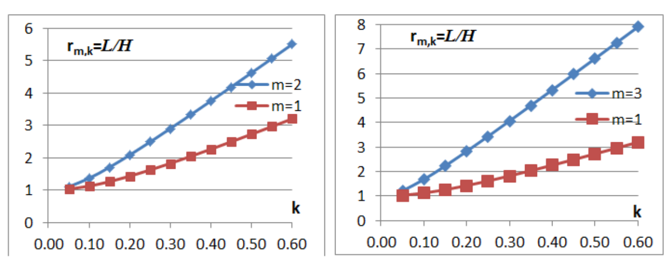

Fig.7 The ratio variation of the lengths of the rope vortex versus the slope $k = \frac{R}{\boldsymbol{H}}$

Table 1

p	L/H, m=1	L/H, m=2
0.5	0.507185963852520	0.53429835534326
0.55	0.557062603118863	0.58373460907019
0.6	0.606854159830626	0.62977408763124
0.65	0.656578287553461	0.68137621750483
0.7	0.706252779187578	0.72973989175682
0.75	0.755895541577370	0.77790676633260
0.8	0.805524569113152	0.82595927970459
0.85	0.855157916514158	0.87398072904834
0.9	0.904813670998359	0.92205496476665
0.95	0.954509924057349	0.97026605984388
1	1.004264743063360	1.01869796334739

If we reconsider that $H = 10$ m, and $R = 0.18$ m, for different values of p, in case of one or two loops of the rope vortex we obtains the values expressed in Table 2.

Reversely, if we consider that L becomes 10 m, then H will be of **9.9575 m** shortened with **0.0425 m** , considering a curve with one loop on the truncated spindle surface.

Table 2.

H (m)	L_1	L_2	$L_1 - H$	$L_2 - H$
5	5.0719	5.2673	0.0719	0.2673
5.5	5.5706	5.7633	0.0706	0.2633
6	6.0685	6.2266	0.0685	0.2266
6.5	6.5658	6.7455	0.0658	0.2455
7	7.0625	7.2328	0.0625	0.2328
7.5	7.5590	7.7184	0.0590	0.2184
8	8.0552	8.2029	0.0552	0.2029
8.5	8.5516	8.6871	0.0516	0.1871
9	9.0481	9.1715	0.0481	0.1715
9.5	9.5451	9.6568	0.0451	0.1568
10	10.0426	10.1437	0.0426	0.1437

Table 3.

p	0.6	0.65	0.7	0.75	0.8	0.85	0.9	0.95	1
L	6.0	6.5	7.0	7.5	8.0	8.5	9.0	9.5	10.0
H_1	5.9322	6.4349	6.9380	7.4415	7.9451	8.4487	8.9521	9.4551	9.9575
ΔH_1	0.0678	0.0651	0.0620	0.0585	0.0549	0.0513	0.0479	0.0449	0.0425
H_2	5.7816	6.2634	6.7747	7.2878	7.8021	8.3169	8.8317	9.3457	9.8583
ΔH_2	0.2184	0.2366	0.2253	0.2122	0.1979	0.1831	0.1683	0.1543	0.1417

CONCLUSIONS

If the base flow containing a strong vortex which counter-rotates the runner, to control the vortex rope, the tangential components of the jets are positive (see [1]). If the base flow containing a strong vortex which co-rotates with the runner, to control the vortex, the tangential components of the jets are set negative (see [1]).

The flow control with different momentum fluxes, translated in column of the water, affects the size of the vortex rope. Correlation between jet type, high of the column of the water and the lenght of the vortex rope were made. The calculus could be used for modernization of the hidraulic laboratory for simulations.

Given the experimental data obtained for the rope vortex as curve on cone surface in [5], the length of the rope was computed. The numerical value of the rope length obtained by an analytical calculus for the experimental curve mentioned was used in order to find the dimension of the spindle magnitude as function of the rope loops. This value could be useful in real life in both cases, if we know the magnitude and determining the number of the curve loops or reversely, in the most encountered cases.

ACKNOWLEDGEMENTS

This work presented has been founded by University Politehnica of Bucharest, through the “Engineer in Europe” Programme.

REFERENCES

[1] Javadi A., Nilsson H., Active Flow Control of the Vortex Rope and Pressure Pulsations in a Swirl Generator, Engineering Applications of Computational Fluid Mechanics, DOI: 10.1080/19942060.2016.1235515, 2016

[2] Baoshan Zhu, Hong Wang, Longbu Wang, Shuliang Cao, Three - dimensional vortex simulation of unsteady flow in hydraulic turbines, International Journal for Numerical Methods in Fluids, Volume 74, Issue 2, page 152, 20 January 2014.

[3]Bosioc A.I., Resiga R., Muntean S., Tanasa C., Unsteady Pressure Analysis of a Swirling Flow With Vortex

Rope and Axial Water Injection in a Discharge Cone, Journal of Fluids Engineering, 2012, DOI: 10.1115/1.4007074

[4] Baran G., Ciocanea A. – Curgeri cavitationale si abrazive, Editura Printech, Bucuresti, 2005, pp.59-93.

[5] Ciocan G. D., Iliescu M. S., Vu T. C., Nennemann B. and Avellan F. 2007 Experimental Study and Numerical Simulation of the FLINDT Draft Tube Rotating Vortex J. Fluids Eng. 129.,pp. 146-58.

[6] Hosein Foroutan, Savas Yavuzkurt, Flow in the Simplified Draft Tube of a Francis Turbine Operating at Partial Load—Part I: Simulation of the Vortex Rope, Journal of Applied Mechanics, DOI: 10.1115/1.4026817,Vol 81, 2014, http://appliedmechanics.asmedigitalcollection.asme.org/

[7] Kuibin P. A., Okulov V. L., Susan-Resiga R. F., Muntean S. Validation of mathematical models for predicting the swirling flow and the vortex rope in a Francis turbine operated at partial discharge, 2010, IOP Conf. Ser.: Earth Environ. Sci. 12 012051, (http://iopscience.iop.org/1755-1315/12/1/012051).

[8] Kurosava S., Satou S. Turbulent Flow Simulation for the draft tube of a Kaplan Turbine, 23rd IAHR Symposium, Yokohama, October 2006.

[9] PASCHE S., Dynamics and Optimal Control of Self-Sustained Instabilities in Laminar and Turbulent Swirling Flows: Application to the Part Load Vortex Rope in Francis Turbines, thèse no 8363, École Polytechnique Fédérale de Lausanne, 2018.

[10] Susan-Resiga R., Vu T., Muntean S., Ciocan G.D., Nennemann B. Jet control of the Draft Tube Vortex Rope in Francis Turbines at Partial Discharge, 23rd IAHR Symposium, Yokohama, October 2006.

[11] Susan-Resiga R., Muntean S., Stein P., Avellan F. Axisymmetric Swirling Flow Simulation of the Draft Tube Vortex in Francis Turbines at Partial Discharge Int. J. Fluid Mach. and Sys., 2(4) 295-302 , 2009 .

[12] Zhow L., Wang Z., Tian Y. – Numerical Simulation of Vortex Cavitation in Draft Tube, 23rd IAHR Symposium, Yokohama, October, 2006.

[13] Weili L., Phengcheng G., Xingqi C., Xiaobo Z., Jinglin L. Numerical investigation of flow characteristics in a Francis turbine, IAHR 24th Symposium on Hydraulic Machinery and Systems, October 27-31, Foz do Iguassu, 2008.